Development 120, 2015-2025 (1994)
Printed in Great Britain © The Company of Biologists Limited 1994

Morphogenesis of *Drosophila* ovarian ring canals

Douglas N. Robinson, Kelly Cant and Lynn Cooley

Department of Genetics, Yale University School of Medicine, 333 Cedar Street, New Haven, CT 06510, USA

SUMMARY

We analyzed the structure of cytoplasmic bridges called ring canals in *Drosophila* egg chambers. Two mutations, *hu-li tai shao* (*hts*) and *kelch*, disrupt normal ring canal development. We raised antibodies against the carboxy-terminal tail of hts and found that they recognize a protein that localizes specifically to ring canals very early in ring canal assembly. Accumulation of filamentous actin on ring canals coincides with the appearance of the hts protein. kelch, which is localized to the ring canals hours after hts and actin, is necessary for maintaining a highly ordered ring canal rim since *kelch* mutant egg chambers have ring canals that are obstructed by disordered actin and hts. Anti-phosphotyrosine antibodies immunostain ring canals beginning early in the germarium before hts and actin and throughout egg chamber development. The use of antibody reagents to analyze the structure of wild-type and mutant ring canals has shown that ring canal development is a dynamic process of cytoskeletal protein assembly, possibly regulated by tyrosine phosphorylation of some ring canal components.

Key words: *Drosophila*, oogenesis, ring canals, *kelch*, *hu-li tai shao*

INTRODUCTION

Cells use a number of mechanisms to communicate with one another during development. These mechanisms include secretion of diffusible ligands, secretion of extra-cellular matrix, and the formation of adherens and gap junctions upon contact with each other. During gametogenesis of several vertebrate and invertebrate organisms, an unusual type of intercellular communication is used. As a result of incomplete cytokinesis during mitotic divisions, gametes of males and females develop as syncytia connected by large cytoplasmic bridges called ring canals (Burgos and Fawcett, 1955; Brown and King, 1964). In mammals, syncytial development may be required to synchronize mitotic divisions and entry into meiosis and possibly to synchronize atresia or selective degeneration of oocytes (Franchi and Mandl, 1962; Weakley, 1967; Zamboni and Gondos, 1968; Dyer et al., 1968; reviewed by Gondos, 1973). During oogenesis of many insects, the cytoplasmic bridges allow the flow of nutrients between cells in a syncytium. Only one cell develops into a mature oocyte while the other cells retract and die after contributing their cytoplasmic contents to the oocyte (King and Mills, 1962; Mahowald and Kambysellis, 1980; Anderson and Huebner, 1968). In *Drosophila* oogenesis, cytoplasm transport between nurse cells and the oocyte is essential for the development of a normal oocyte (Mahowald and Kambysellis, 1980; Spradling, 1993 for reviews of *Drosophila* oogenesis). The cytoskeleton plays an integral role in cytoplasm transport because disruption of the cytoskeleton by mutation (Storto and King, 1988; Cant et al., 1994; Cooley et al., 1992) or by pharmacological agents (Gutzeit, 1986a,b; Theurkauf et al., 1993) causes defective transport. Cytoplasm transport also depends on a class of specialized cytoskeletal proteins that are required for development of a functional ring canal during *Drosophila* oogenesis.

The *Drosophila* ovary consists of 15-18 discrete tubular ovarioles (Fig. 1A). The germline stem cells reside at the anterior of each ovariole in the germarium (Fig. 1B). In region 1 of the germarium, stem cell daughters undergo four rounds of mitosis with incomplete cytokinesis. This gives rise to 16-cell clusters in which two cells have 4 intercellular bridges, two cells have three, four cells have two, and eight cells have one. One of the 16 cells differentiates into the oocyte while the other fifteen differentiate into the nurse cells (Fig. 1C). In germarium region 2a, newly formed 16-cell clusters are enclosed by migrating follicle cells forming the egg chamber, and in region 2b the egg chambers become lens-shaped. Region 3 contains stage 1 spheroidal egg chambers that are ready to enter the vitellarium for maturation (Brown and King, 1964; Koch and King, 1966; Mahowald and Strassheim, 1970). In the vitellarium, progressively more mature egg chambers extend from the anterior to the posterior end of the ovariole. These egg chambers have been divided into stages 2-14 where a stage 14 oocyte is ready to be fertilized and oviposited.

Cleavage furrow arrest and ring canal development are not well understood. Early studies using electron microscopy revealed a highly vesiculated structure called fusome extending through the cytoplasmic bridges, possibly functioning to stabilize the cleavage furrow until a ring canal is established (Meyer, 1961; Koch and King, 1966; King and Storto, 1988; Lin et al., 1994). Similar studies also revealed that when a ring canal is formed, two components are added sequentially. First, an electron opaque backbone that is a part of or adjacent to the plasma membrane is added upon arrest of the cleavage furrow. Second, an electron dense inner rim accumulates after the final mitotic division of each germline syncytia (Fig. 1D;

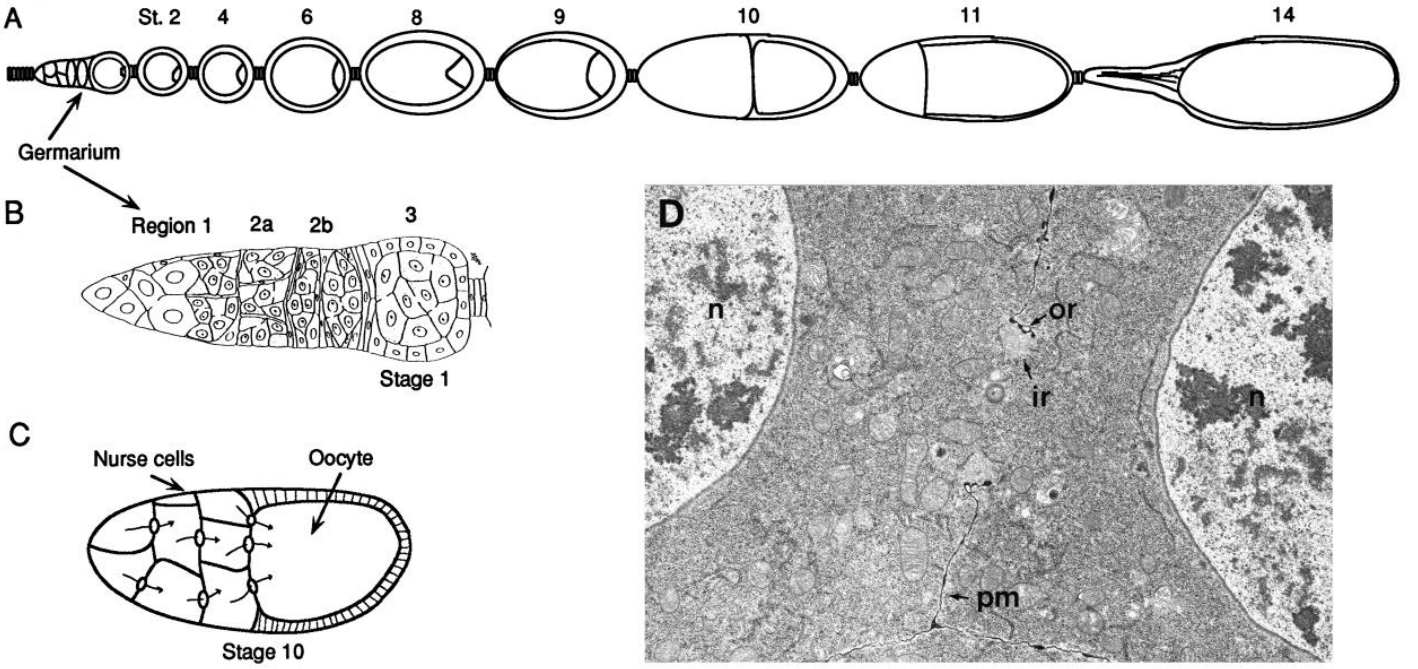

Fig. 1. Ring canals in *Drosophila* oogenesis. (A**)** The *Drosophila* ovary is divided into discrete units called ovarioles. An ovariole (shown schematically here) has a germarium at the anterior end anchored by a terminal filament. Progressively more mature egg chambers move posteriorly until the most mature oocyte (stage 14) is fertilized and oviposited. St. = stage. **(**B**)** The germarium (germarium picture adapted from Mahowald and Strassheim, 1970) of a *Drosophila* ovariole has been divided into regions 1, 2a, 2b, and 3 (Mahowald and Strassheim, 1970; Koch and King, 1966). Region 1 contains germline stem cells and mitotically active 2-, 4-, and 8-cell clusters. Clusters of 16 germline cells are present in 2a where follicle cells begin to migrate around the cluster. Young egg chambers completely surrounded by follicle cells flatten into a lens shape in region 2b. The egg chamber reaches region 3 of the germarium (stage 1) where it becomes spherical and prepares for departure from the germarium as a stage 2 egg chamber. (C) Maternal components are transported from the nurse cells to the oocyte through the ring canals during oogenesis. Transport begins as early as germarium region 2. When the egg chambers reach stage 10, a final, rapid phase of cytoplasm transport begins in which the remaining contents of the nurse cells are transported into the oocyte. (D) An electron micrograph of a ring canal interrupting the plasma membrane (pm) between two nurse cells is shown. The ring canal is made of an electron opaque outer rim (or) and an electron dense inner rim (ir). The canal is large enough for components as large as mitochondria to pass through the opening. n, nucleus.

Meyer, 1961; Koch and King, 1969; Mahowald, 1971). The inner rim is established coordinately with the degeneration of the fusome (Koch and King, 1969; Lin et al., 1994) and the addition of actin to the ring canal (Warn et al., 1985; Theurkauf et al., 1993).

The genes for two mutations, *hu-li tai shao* and *kelch*, which either disrupt ring canal structure or cytoplasm transport have been cloned. Mutants for *hu-li tai shao* (*hts*) (Yue and Spradling, 1992) produce degenerate ovaries that contain egg chambers with less than a full complement of germline cells. Frequently, an oocyte fails to differentiate in these mutant egg chambers. In addition, mutant egg chambers do not accumulate the inner rim of ring canals and have no actin on their ring canals (Yue and Spradling, 1992). The known *hts* cDNA predicts a protein that is 37% identical to adducin in the amino-terminal globular region, hinge region and the first part of the adducin tail domain. hts protein and adducin share no homology in the final 160 amino acids of adducin, and hts contains an additional 400 amino acids (carboxy-terminal tail) not found in adducin (Fig. 2; Yue and Spradling, 1992; Ding et al., 1993).

Mutants for *kelch* fail to complete cytoplasm transport from the nurse cells into the oocyte resulting in a female sterile phenotype. Cytoplasm transport is affected beginning early in the vitellarium where oocytes in mutant egg chambers are smaller than wild-type oocytes of the same stage (Xue and Cooley, 1993). The *kelch* gene was cloned and found to encode a protein specifically localized to ring canals (Xue and Cooley, 1993). The kelch protein contains two motifs found in several other proteins (Koonin et al., 1992). The first motif is a 100 amino acid domain called the BTB box (Godt et al., 1993) that is positioned approximately 150 amino acids from the amino terminus. The BTB box is found at the amino terminus of several *Drosophila* transcription factors including Broad-Complex (DiBello et al., 1991), Tramtrack (Harrison and Travers, 1990), and Adf2 (Benyajati, personal communication). Several open reading frames (ORFs) in a number of Pox viruses (Koonin et al., 1992; Senkevich et al., 1993) also contain the BTB box. The function of the BTB box is unknown. The second motif consists of six 50 amino acid repeats called kelch repeats. The Pox virus ORFs (Koonin et al., 1992; Senkevich et al., 1993), mouse MIPP (Chang-Yeh et al., 1991), and scruin protein (Tilney, 1975) from *Limulus* contain several kelch repeats (Way and Matsudaira, personal communication).

We present studies on the formation of functional ring canals

and ring canal structure in *hts* and *kelch* mutants. This work has relied on several antibody reagents including new antibodies raised against the carboxy-terminal tail of hts that specifically recognize ring canals and anti-phosphotyrosine antibodies that recognize one or more additional components of a ring canal. The proteins are added sequentially to the arrested cleavage furrow during ring canal ontogeny. These results have allowed us to formulate a model of ring canal structure and to speculate on the early events necessary to stabilize and transform an arrested cleavage furrow into a ring canal.

MATERIALS AND METHODS

Fly strains

w^{1118} or *cn; ry* (Lindsley and Zimm, 1992) flies were used as wild type in these experiments. hts^{1} mutant flies have been described previously by Yue and Spradling (1992). kel^{neo} mutant flies were described previously by Xue and Cooley (1993). Fly stocks were maintained under standard conditions.

Antibody production

Monoclonal antibodies to the carboxy-terminal tail of hts were generated using standard procedures. Recombinant fusion proteins were made using the pGEX system (Smith and Johnson, 1988). A *Bgl*II-*Eco*RI fragment from htsc5 (Yue and Spradling, 1992) encoding the carboxy-terminal 351 amino acids (Fig. 2) was cloned into pGEX-2T. Protein was produced as a fusion to the carboxy terminus of *Schistosoma japonicum* glutathione-S-transferase (Sj26) and purified from inclusion bodies. Purified protein was injected into mice and hybridoma cell lines were generated according to Harlow and Lane (1988). Antisera and hybridoma cell line supernatants were screened for immunoreactivity to the fusion protein and to wild-type but not hts^{1} mutant ovaries.

Western analysis

Drosophila ovaries were dissected in *Drosophila* Ringer's solution and ground in 1× Laemmli's buffer under reducing conditions (Laemmli, 1970). Protein concentrations of the ovary extracts were measured using the BioRad Protein Assay. Proteins separated by SDS-polyacrylamide gel electrophoresis (Laemmli, 1970) were transferred to Hybond-ECL nitrocellulose (Towbin et al., 1979; Amersham). Following transfer, membranes were blocked in Blotto-Tween (5% powdered milk, 0.2% Tween, and PBS) for 2 hours, then incubated in hybridoma cell supernatant (1:10 in Blotto-Tween) for 1 hour to overnight. Membranes were washed four times for 10 minutes each in 0.2% Tween in PBS at room temperature. Membranes were incubated for 30 minutes at room temperature in goat anti-mouse IgG secondary antibody conjugated to horseradish peroxidase (Pierce Chemical Co.) in Blotto-Tween (1:10,000). After four washes, signals were detected using ECL western blotting detection reagents (Amersham) according to manufacturer's specifications.

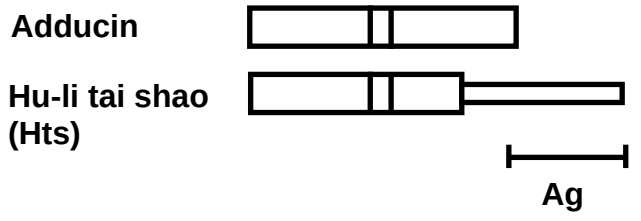

Fig. 2. hts cDNA structure. Schematic diagram showing the relationship between the predicted product of the *hts* cDNA and adducin. The larger box corresponds to the adducin homology region that is divided into the amino-terminal globular domain, a small hinge domain (small internal box), and a carboxy-terminal tail. The narrow box corresponds to the region of hts that is unrelated to known proteins. Mouse monoclonal antibodies were generated against a recombinant carboxy-terminal antigen (Ag).

Immunolocalization and confocal imaging

Whole ovaries were dissected in *Drosophila* Ringer's, fixed in 1% formaldehyde saturated with heptane (Cooley et al., 1992), washed three times for 10 minutes in PBS and once for 10 minutes in PBT (0.3% Triton X-100 (Sigma), 0.5% BSA (Sigma) in PBS) at room temperature. For actin visualization, ovaries were incubated in 2-4 units of rhodamine-conjugated phalloidin (Molecular Bioprobes) for 20 minutes at room temperature. For antibody staining, ovaries were incubated in hts carboxy-terminal antibody hybridoma supernatant (1:1), kelch hybridoma supernatant (Xue and Cooley, 1993) (1:1), or anti-phosphotyrosine antibody (UBI, 4G10 or ICN Biochemicals, PY20) (1:1000) diluted in PBT. The ovaries were incubated with rocking for 2 hours at room temperature then overnight at 4°C. After washing four times for 15 minutes in PBT, bound antibodies were detected using a goat anti-mouse IgG secondary antibody conjugated to fluorescein isothiocyanate (Jackson Laboratories). Immunolocalizations were visualized by collecting 1-2 μm optical sections on a laser-scanning confocal microscope (BioRad MRC 600) and compiling and displaying optical sections using the CoMOS software package (BioRad). Either a 50× (0.95 NA) or a 100× (1.30 NA) objective was used in each case.

RESULTS

Temporal order of hts, actin, and kelch addition to ring canals

To study the role of the *hts* gene in the development of *Drosophila* egg chambers, we generated mouse monoclonal antibodies against the carboxy-terminal 351 amino acids (carboxy-terminal domain) of hts (Fig. 2). By western analysis, the monoclonal antibodies recognized a doublet of proteins with apparent relative molecular masses of approximately 60×10^{3} M_{r} (Fig. 3A). Both bands were present in wild-type and kel^{neo} ovary extracts but were absent in hts^{1} mutant extracts. The monoclonal antibodies specifically immunostained ring canals (Fig. 3B). Ring canal staining was first apparent in region 2a of the germarium (see Fig. 4) and persisted on the ring canals until stage 13 (not shown). Antibody staining was reduced or absent in *hts* mutants depending on the severity of the *hts* allele examined (not shown). When there was protein present in weak *hts* mutants, it localized to abnormal ring canals.

Localization of actin, hts, and kelch showed a distinct temporal order to their recruitment to ring canals (Fig. 4). Actin was first seen on ring canals beginning in region 2a (Fig. 4A; Theurkauf et al., 1993). hts also began accumulating on ring canals at this time (Fig. 4B). To verify that actin and hts appear at ring canals simultaneously, double labeling with anti-hts antibodies and rhodamine-conjugated phalloidin was performed (Fig. 4C). All of the ring canals appeared yellow indicating that hts (green) and actin (red) arrived on the ring canals at the same time. Finally, kelch localization to ring canals began in region 3 of the germarium. Initially, the kelch staining pattern was on a subset of ring canals, and all ring canals were labeled by stage 3 (Fig. 4D).

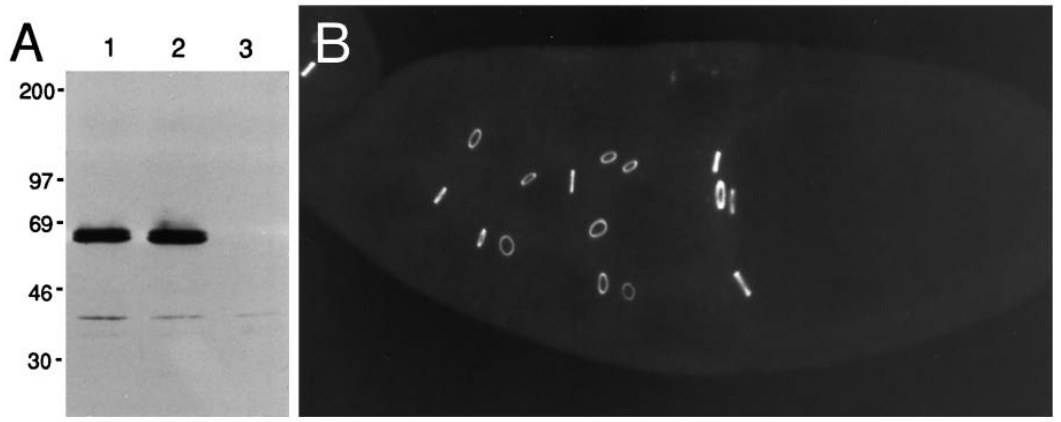

Fig. 3. Antibodies raised against the hts carboxy-terminal tail specifically immunostain ring canals. (A) A hts monoclonal antibody recognizes a doublet of protein bands with an apparent relative molecular mass of approximately 60×10^3 M_r in wild-type and kelch mutant ovary extracts (lanes 1 and 2, respectively). Both proteins are absent in *hts*^{1} mutant ovary extracts (lane 3). A lower molecular weight protein is also recognized; however, it is also present in *hts*^{1} mutant ovary extracts. 20 μg of protein were loaded per lane. (B) Monoclonal antibodies raised against the carboxy-terminal tail of hts immunostain ring canals in *Drosophila* egg chambers. A stage 10 egg chamber is shown.

Anti-phosphotyrosine antibodies identify another component of ring canals

A number of colleagues informed us that anti-phosphotyrosine antibodies immunostain ring canals. Indeed, immunostaining of ovaries with anti-phosphotyrosine antibodies showed strong staining of all 15 ring canals as well as a lower level staining on membranes and in cytoplasm (Fig. 5A). We refer to the protein or proteins identified by the anti-phosphotyrosine antibodies as phosphotyrosine protein. The anti-phosphotyrosine immunostaining of ring canals began in the germarium (Fig. 5B,C). Ring canal staining was observed as early as late region 1 when the germline syncytia are undergoing their final round of mitosis (Fig. 5C). The phosphotyrosine staining increased in amount on the ring canal by region 2a when actin and hts were first seen on the ring canals (Fig. 5B, arrow; Fig. 4). *hts*^{1} mutant ring canals that lack the electron dense inner rim (Yue and Spradling, 1992) still stained with the anti-phosphotyrosine antibodies (Fig. 5D). Anti-phosphotyrosine antibodies recognized several bands on western blots of wild-type and *hts*^{1} mutant ovary protein extracts (not shown) indicating that there may be several phosphotyrosine proteins involved in ring canal development.

kelch is a structural component of ring canals

The localization of kelch protein to the ring canal beginning in region 3 of the germarium (Fig. 4D) suggested that kelch is not involved in the initial establishment of the ring canal. To investigate its role in ring canal structure, we used anti-hts antibodies and actin staining to examine ring canal structure in *kelch* mutants. Comparison of hts protein localization in wild-type and *kelch* mutant germaria suggested that the *kelch* mutant ring canals were morphologically normal in these early stages. The wild-type and mutant hts protein pattern resembled a tire rim with a concave outer face (Fig. 6A,B). The canal had a diameter of approximately 0.5 μm whereas the outer diameter of the ring was 1-2 μm. In wild-type stage 4 egg chambers, hts was localized in very thin bands with concave outer faces similar to the pattern found in germaria (Fig. 6C). The canal pore was completely devoid of hts protein and had a diameter ranging between 2-3 μm depending on position of the ring canal in the egg chamber. The rings visualized by anti-hts antibodies in *kelch* mutants also had a concave outer face, but the organization was more diffuse. Many canals appeared to be occluded by diffusely distributed hts protein reducing the diameter to 0.5-2 μm (Fig. 6D). By stage 10 in wild-type egg chambers, the anti-hts staining pattern revealed rings with a smooth appearance forming a highly organized band that was slightly concave on the outer face (Fig. 6E). The inner diameter of the wild-type ring was approximately 6-7 μm and the outer diameter ranged from 7-8 μm. In stage 10 *kelch* mutant egg chambers, hts antibodies revealed rings that were severely disorganized with hts protein diffusely distributed through the canal (Fig. 6F). The concavity of the outer face of the rim was completely absent, and the inner diameter of the canal was reduced to approximately 2 μm. The anti-hts immunofluorescence pattern in these late stage *kelch* mutant ring canals appeared to be more intense either due to greater abundance of hts protein on the ring canal or due to greater availability of antibody epitopes.

The organization of actin in the ring canals was also disrupted in *kelch* mutants. In wild-type stage 7-8 egg chambers, the actin localized to a tight band of protein embedded in the subcortical actin meshwork (Fig. 6G). Wild-type actin rings at this stage had an outer diameter of 5-6 μm and an inner diameter of approximately 4 μm. In *kelch* stage 7-8 egg chambers, the actin ring had an outer diameter of 5-6 μm but an inner diameter of only 1 μm (Fig. 6H). In some *kelch* mutant egg chambers, the actin appeared to form a smaller ring suspended within the lumen of the canal by bundles of actin extending from the thick outer ring of actin (Fig. 6H). In wild-type stage 10 egg chambers, the actin ring formed a tightly ordered band or ring of protein with dimensions similar to the wild-type stage 10 hts protein ring (compare Fig. 6E, I). In stage 10 *kelch* mutant egg chambers, the actin ring was diffuse and extended into the canal (Fig. 6J). Actin staining also appeared to be more intense in *kelch* mutant ring canals than in the wild-type counterparts. Like the anti-hts staining, this may signify an increase in the amount of filamentous actin on the *kelch* mutant ring canal or a greater availability of phalloidin binding sites. Despite the altered actin organization in ring canals, cytoplasmic actin bundles still formed in stage 10 *kelch* mutant egg chambers (Fig. 6J arrowhead; Xue and

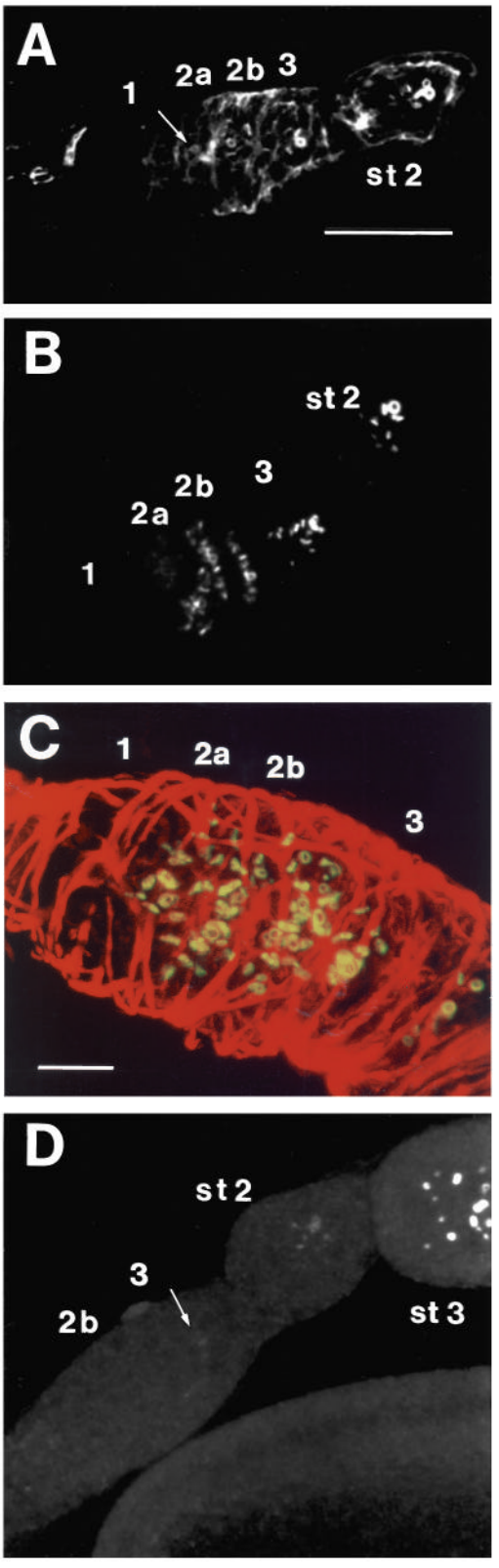

Fig. 4. Actin and hts are localized to ring canals beginning in germarium region 2a; kelch is recruited hours later beginning in region 3. (A) Actin localization to the ring canals begins in late region 2a (arrow) of the germarium. Subcortical actin is present in various other structures including the follicle cell layer, and germline cells in the egg chamber. Note the absence of filamentous actin in region 1. Scale bar, 30 μm. (B) Localization of the hts protein to ring canals also begins in region 2a. The hts antibody very specifically identifies an epitope on the ring canal. Magnification same as in A. (C) Double-labeling of germaria with anti-hts antibodies (green) and with rhodamine-conjugated phalloidin (red) show that hts and actin recruitment to ring canals begins simultaneously in region 2a. The co-localized protein staining pattern appears yellow. Scale bar, 10 μm. (D) kelch protein is detectable on ring canals beginning in region 3 of germaria (stage 1 egg chambers) (arrow). However, it does not become detectable on all ring canals until stage 3. Magnification same as in A.

Cooley, 1993). It appears that kelch functions to organize only the actin in ring canals and does not play a role in actin organization in other parts of the egg chamber.

Cross-sectional view of ring canals

Immunofluorescence of hts protein in early to mid-stage wild-type and *kelch* mutant egg chambers (Fig. 6) showed that hts forms a tire rim-shaped ring of protein. To assess the relationship between hts and actin, double labeling of wild-type ring canals for hts and actin was performed. A cross-sectional view of labeled stage 4-5 ring canals showed different localization patterns for hts and actin. A cross-sectional view of a tire rim appears as two horseshoes with the concave sides facing away from each other. hts staining appeared as horseshoes having a concave outer face (Fig. 7A, arrows). The cross-sectional view of actin in the same ring canal rim was globular rather than horseshoe-shaped (Fig. 7B, arrowheads). The merged image of the two immunofluorescence patterns showed that hts and actin largely co-localized but that the actin filled in the horseshoe (Fig. 7C).

Ring canal protein distribution

Double-labeling experiments with combinations of anti-phosphotyrosine, anti-hts, anti-kelch, and rhodamine-conjugated phalloidin provided further insight into the structure of the ring canal. Since the phosphotyrosine protein was found on ring canals before hts and actin and was present in *hts*^{1} mutant egg chambers, we predicted that phosphotyrosine protein might be found exclusively at the outer-most rim of wild-type ring canals. Instead, double-labeling for phosphotyrosine protein and actin showed that the proteins appeared to co-localize throughout the inner rim (Fig. 8A-B). The phosphotyrosine protein at the outer rim may also be associated throughout the actin layer or there may be additional phosphotyrosine-containing proteins distributed in the inner rim. Double-labeling with anti-hts antibodies and rhodamine-conjugated phalloidin showed nearly complete overlap of actin and hts (yellow) with an enrichment of hts (green) to the inner surface of the actin (red) in ring canals in stage 3-6 egg chambers (Fig. 8C-E). Double-labeling for kelch and actin also showed an enrichment of kelch toward the inner surface of stage 3-6 ring canals with nearly complete overlap between kelch and actin (Fig. 8F). In older stage 9 and 10 egg chambers, the phosphotyrosine, actin, hts, and kelch proteins compacted so that total overlap was observed (Fig. 8G).

DISCUSSION

Formation of a ring canal involves sequential recruitment of

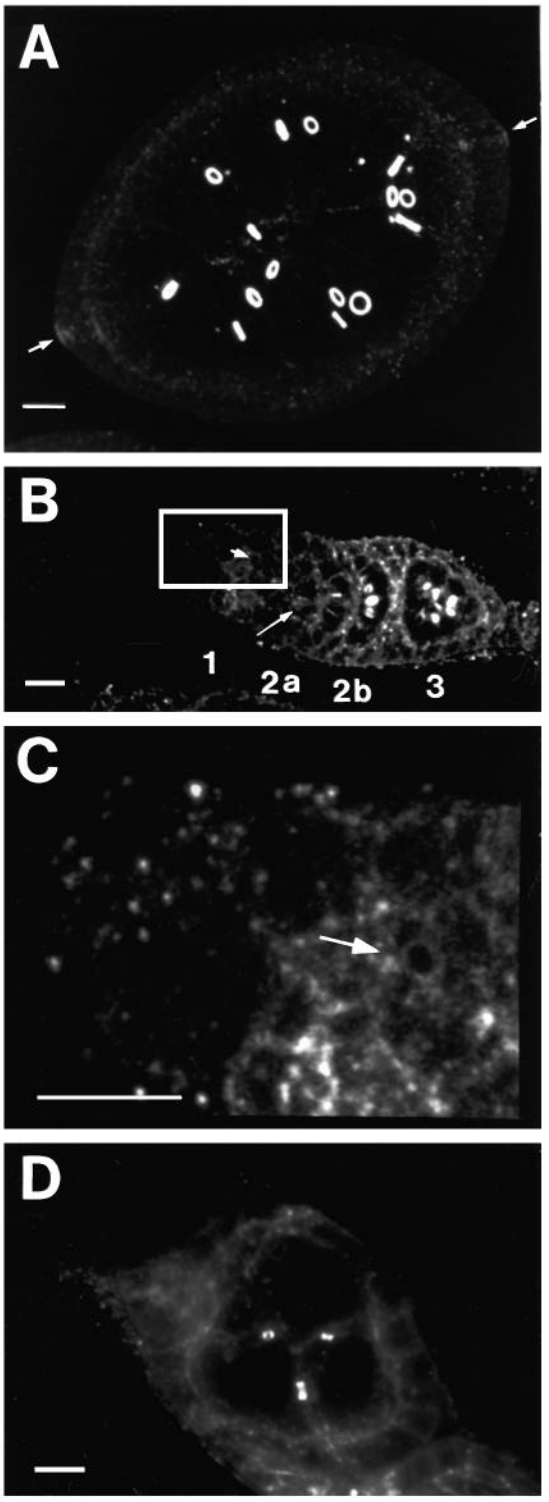

Fig. 5. A phosphotyrosine-containing protein is found on ring canals. (A) Anti-phosphotyrosine antibodies intensely immunostain ring canals in egg chambers of all stages (stage 5-6 egg chamber shown). Less intense staining is present elsewhere in the egg chamber including the anterior and posterior follicle cells (arrows). (B,C) Anti-phosphotyrosine antibodies stain ring canals very early in the germarium. Ring canals are readily identified in region 2a (large arrow), 2b, and 3. Tiny rings are visible in late region 1, just prior to when actin and hts begin to be localized to ring canals. The image in C is a magnified view (4×) of the boxed region in region 1 in B. Arrow in C identifies a late region 1 ring canal. (D) In *hts*^{1} mutant egg chambers, the cytoplasmic bridges are immunostained by anti-phosphotyrosine antibodies. In this stage 4 egg chamber, there were only three ring canals. Scale bars, 10 μm.

several proteins during germarial stages of development and dynamic rearrangement of overall ring canal rim structure during ring canal growth. By late germarium region 1 where 8-cell clusters are present, at least one phosphotyrosine protein can be detected on the ring canals. hts and actin are recruited to the ring canal shortly after the mitotic divisions are complete in region 2a. Finally, kelch is organized in ring canals beginning in region 3 of the germarium and is necessary to maintain the compaction of hts and actin in the inner rim of the ring canal. The sequential recruitment of components to the ring canal is consistent with the ultrastructure of developing ring canals. The electron opaque outer rim is established as the cleavage furrows are arrested, and the electron dense inner rim is added after the completion of the fourth mitotic division in region 2 of the germarium (Yue and Spradling, 1992).

Since a ring canal consists of two domains with different electron densities when viewed by electron microscopy, one would predict that the chemical makeup of the two domains would be different. Koch and King (1969) determined that the outer rim contained glycoproteins by staining with periodic acid/Schiff reagent, whereas the inner rim stained only with fast green at pH 2 indicating that it is made of polysaccharide-free proteins. Our immunocytochemistry experiments allow us to define further the nature of the proteins of the inner and outer rims (Fig. 9). In our model, at least one phosphotyrosine protein is adjacent to or associated with the membrane and is part of the outer rim (Fig. 9A). This or other phosphotyrosine proteins are also distributed through the actin domain of the ring canal. Actin is a component of the inner rim since its absence from the ring canal corresponds with the absence of the inner rim (Yue and Spradling, 1992). hts and kelch are distributed in the actin domain being enriched toward the inner most face of the ring canal rim in young egg chambers (Fig. 9B). By later stages, the ring canal rim is compacted, and actin, phosphotyrosine protein, hts, and kelch are all co-localized (Fig. 9C). Compaction of the inner rim between early stage ring canals and stage 9-10 ring canals can also be observed by electron microscopy (Yue and Spradling, 1992). Proper compaction depends on the presence of the kelch protein since in its absence, the ring canal is disorganized and nearly occluded by hts and actin. In addition to compacting during growth of the egg chamber, the ring canal grows from 1 μm in diameter in region 1 of the germarium (Fig. 9A) to 7-8 μm in diameter in a stage 10 egg chamber (Fig. 9C). New proteins are added to the ring canal as it develops the inner rim from region 1 of the germarium to stage 3 in the vitellarium. It is not clear whether new addition of protein to the ring canal is required as the ring canal matures from stage 3 to stage 10. Growth might be accomplished by simply rearranging the proteins that are already present on the canal. For example, the actin filaments may slide with respect to one another in order to increase the circumference of the ring canal. However, it is also possible that ring canal growth requires additional actin polymerization and an increase in the other ring canal protein levels.

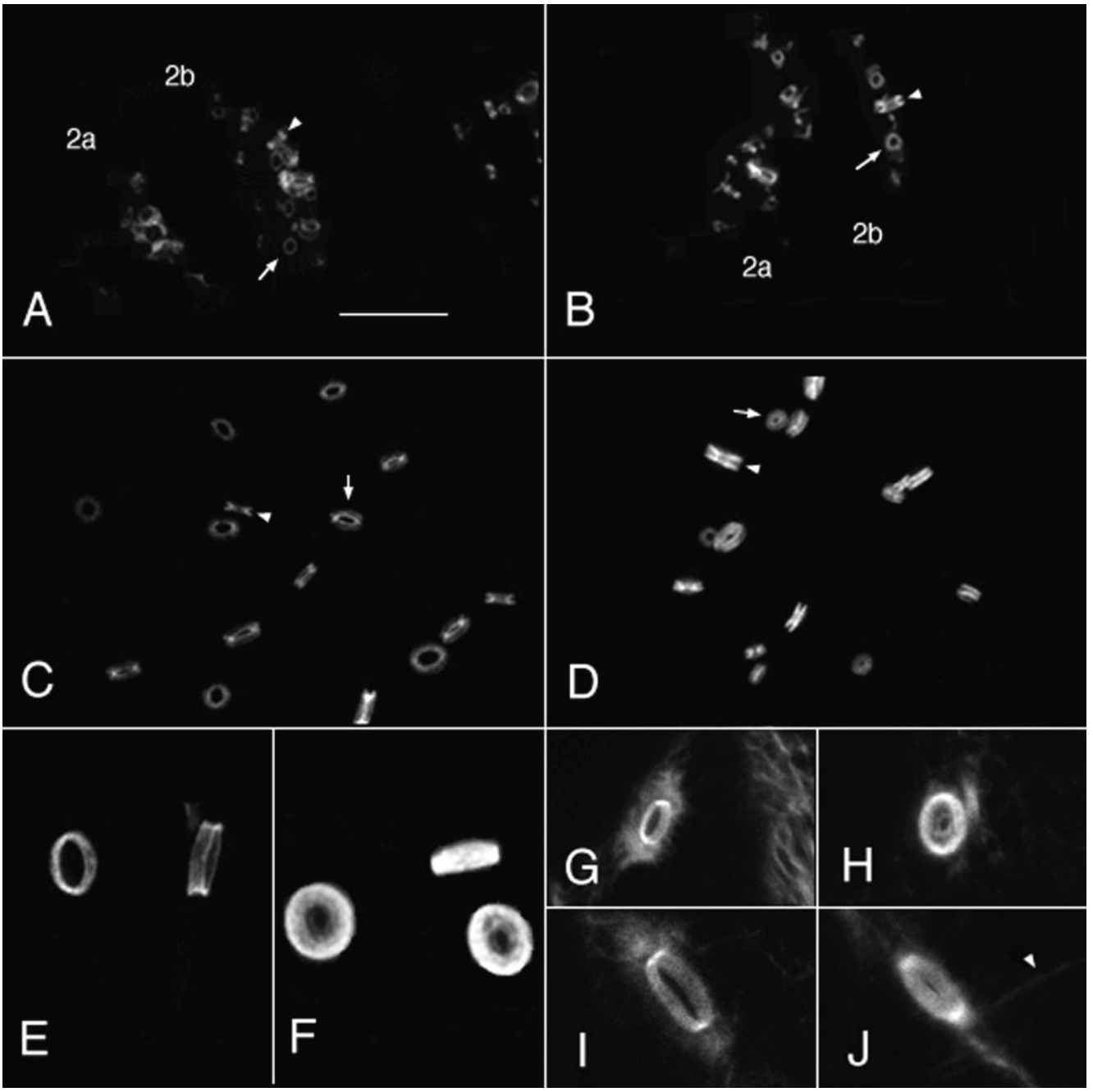

Fig. 6. kelch protein maintains the order of hts and actin in a growing ring canal. Wild type (A) and *kelch* mutant (B) germaria have a similar hts protein immunofluorescence pattern. In wild-type and in *kelch* mutants, the rings stained with hts antibodies are highly organized, forming a band that is concave on the outer face (arrowheads) giving a tire rim appearance. An open canal pore of 0.5 μm is apparent in wild-type and in *kelch* mutant ring canals (arrows). (C) By stage 4, the wild-type rings stained with hts antibodies are highly organized, appearing as thin bands that are concave on the outer face (arrowhead) and that define a wide passageway (2-3 μm) between cells (arrow). (D) In a stage 4 *kelch* mutant egg chamber, the hts protein is more diffuse on the ring canal rim but still forms a concave outer face (arrowhead). The center of the canal is nearly occluded by hts protein (arrow). (E) In wild-type stage 10 egg chambers, the hts protein forms a tightly organized band of protein that is slightly concave. (F) In the *kelch* mutant, the hts protein is localized but very diffuse. It extends into the canal nearly completely obstructing it. The increased brightness of the hts rings of the mutant egg chamber may have been due to increased amount of protein or due to increased epitope accessibility. (G) In wild-type stage 7-8 ring canals, actin forms a tight band of protein with a lumen devoid of filaments. (H) In stage 7-8 *kelch* mutant egg chambers, the shape of actin staining is toroidal rather than in a band as in wild type. In addition, actin is distributed into the canal forming a diffuse array. Sometimes the actin forms a smaller ring within the canal that is connected by actin bundles extending from the outer actin rim. The amount of actin appears to be increased compared to wild type. (I) In wild-type stage 10 ring canals, actin forms a highly organized band of protein similar to the hts protein band at this stage (E). (J) In the *kelch* mutant, actin is diffuse and extends into the lumen of the canal. The defect in actin organization is not general since normal cytoplasmic actin bundles form in stage 10 *kelch* mutant egg chambers (arrowhead). Scale bar, 10 μm for all panels.

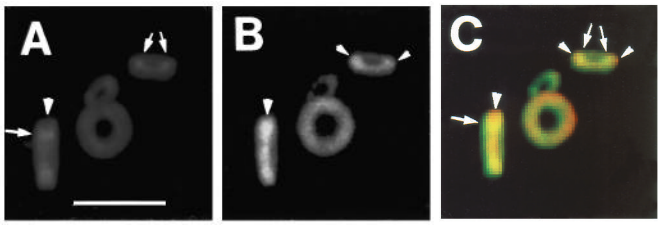

Fig. 7. Cross-sectional views of ring canals showing differential enrichment of proteins in subdomains of the ring canal rim. (A) hts protein staining in wild-type stage 4-5 ring canals appears as a ring of protein that has a concave outer face. A cross-sectional view of the ring canal has the appearance of two horseshoes facing away from each other. The arrows are pointing to the horseshoe, and the arrowhead is pointing to the gap in the horseshoe. (B) Actin staining in the same ring canals is more round or toroidal (arrowheads). (C) A merged image A and B shows that hts (green) is enriched on the inner surface of the ring canal (arrows) and that actin (red) is found filling in the outer region of the ring canal (arrowheads). There is also an extensive zone of co-localization of hts and actin (yellow). Scale bar, 5 μm for all panels.

The role of tyrosine phosphorylation of ring canals proteins remains unknown. Phosphotyrosine proteins have been found in other types of cell-cell and cell-substrate contacts such as adherens junctions and focal adhesions (Volberg et al., 1991, 1992). Treatment of cells with phosphatase inhibitors like H_2O_2/orthovanadate or tyrphostins can cause adherens junction proteins to disassemble and reassemble in focal adhesions suggesting that tyrosine phosphorylation may be an important regulatory event for the formation of these junctions (Volberg et al., 1992). While the relevant targets of these phosphorylation events remain in question, the junctions have proteins in common with cleavage furrows. For example, actin (reviewed by Burridge et al., 1988; Satterwhite and Pollard, 1992) and α-actinin (Fujiwara et al., 1978; Sanger et al., 1987) have been identified in adherens junctions, focal adhesions, and cleavage furrows (reviewed by Satterwhite and Pollard, 1992). Radixin (Tsukita et al., 1989; Sato et al., 1991) has also been identified in adherens junctions and cleavage furrows. In *Drosophila* egg chambers, phosphotyrosine proteins are present in cleavage furrows just prior to the arrival of actin and hts and the accumulation of the inner rim. We speculate that

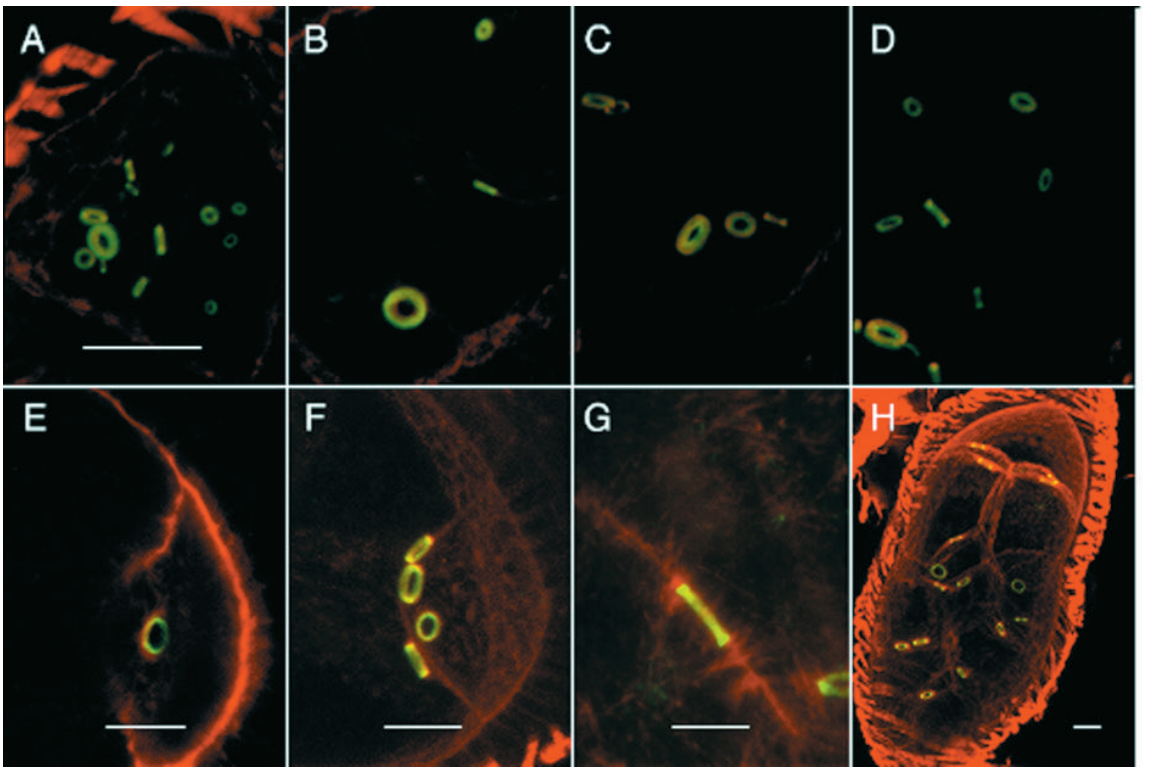

Fig. 8. hts and kelch largely co-localize with actin but show an enrichment on the inner surface of young ring canals. Wild-type stage 3-4 (A) and stage 4-5 (B) ring canals stained with anti-phosphotyrosine antibodies (green) and rhodamine-conjugated phalloidin (red) show considerable overlap (yellow) in the localization pattern. Occasionally, there is a slight enrichment in the anti-phosphotyrosine epitope toward the outer region of the ring. The scale bar in A applies to A-D. (C-E) Wild-type stage 3-4 (C), 4-5 (D), and 6-7 (E) ring canals doubly stained with anti-hts monoclonal antibodies (green) and rhodamine-conjugated phalloidin (red) show an enrichment of hts protein at the inner surface of the ring canal. There is also extensive overlap (yellow) suggesting co-localization of the two proteins. (F) Wild-type stage 6-7 ring canals immunostained with anti-kelch antibodies (green) and rhodamine-conjugated phalloidin (red) show nearly complete co-localization of kelch and actin proteins. There is a small region of green present at the inner surface of the ring canals suggesting an enrichment of the kelch protein on the inner surface. (G) By stages 8-10, double-labeling of wild-type ring canals with anti-phosphotyrosine, anti-hts, or anti-kelch antibodies with rhodamine-conjugated phalloidin shows complete co-localization of the proteins. This is a side view of a stage 10 ring canal double-labeled with anti-kelch antibodies (green) and rhodamine-conjugated phalloidin (red). The ring canal is completely yellow.(H) Actin and kelch co-localize and overlap in all rings of a stage 9 egg chamber. Every ring canal in the egg chamber shows the same pattern of localization of each protein. Scale bars, 10 μm for all panels.

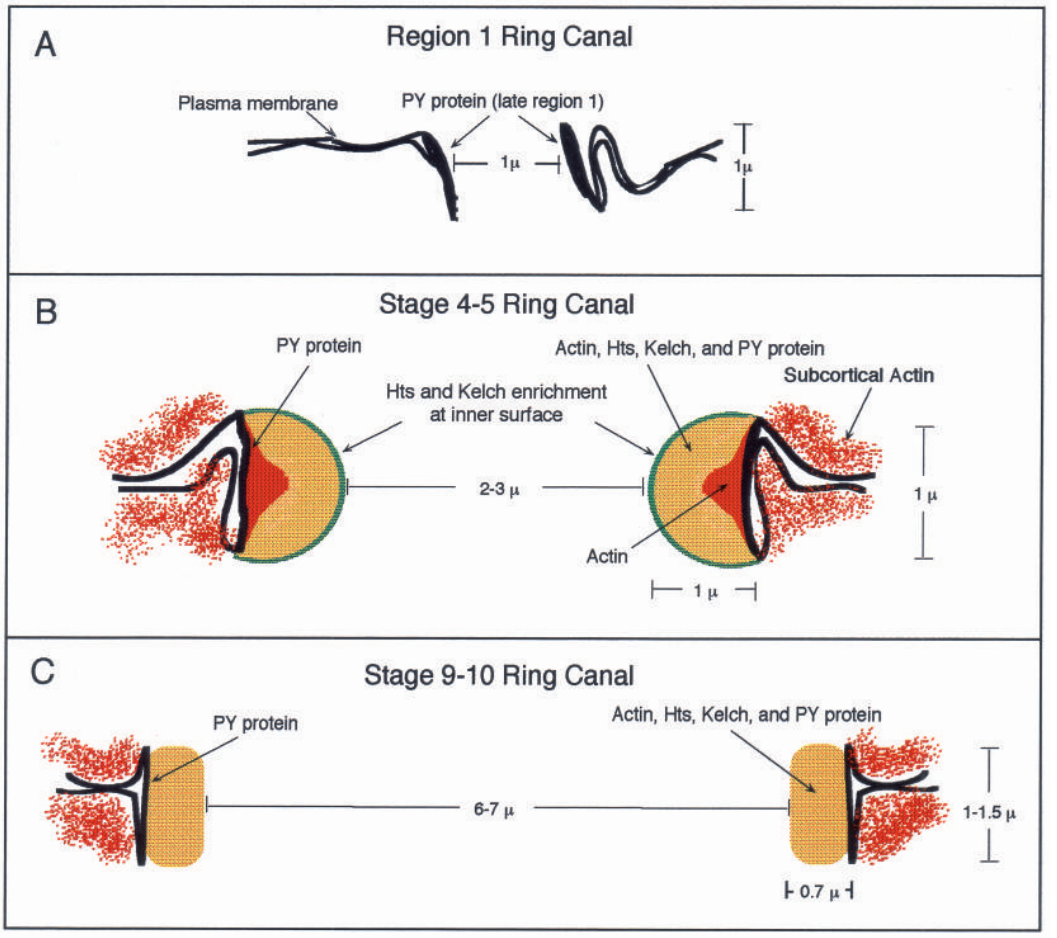

Fig. 9. Model of the structure and development of ring canals. (A) The outer rim of ring canals forms as the cleavage furrows are arrested in region 1 of the germarium. At least one phosphotyrosine protein (PY protein) is present at the cleavage furrow prior to the accumulation of hts and actin on the ring canal. The same or another PY protein is associated with the membranous outer ring canal rim since it is present in *hts*^{1} mutant cytoplasmic bridges that lack the inner rim. (B) By stage 4-5, the inner rim has formed, and hts and kelch proteins are enriched toward the inner surface of the ring canal. Actin is present throughout the inner rim along with hts, kelch, and a phosphotyrosine (PY) protein. (C) All four inner rim proteins co-localize in a compacted band in later stages of egg chambers.

tyrosine phosphorylation of proteins found in cleavage furrows may be necessary to arrest cytokinesis or to initiate the formation of a ring canal. Anti-phosphotyrosine antibodies recognize several protein bands on western blots of whole ovary protein extracts (D. N. R., unpublished data) indicating that there are several candidates for ring canal proteins. Clearly, we need to identify the ring canal phosphotyrosine protein(s) in order to elucidate the role of tyrosine phosphorylation in ring canal development.

The *hts* gene encodes a component of ring canals that is recruited to ring canals at the same time as actin in region 2a of the germarium. Strong mutants for the *hts* gene fail to establish actin on the ring canals and fail to accumulate an inner rim (Yue and Spradling, 1992). Weak mutant alleles for the *hts* gene have a lower level of hts, actin, and kelch proteins on abnormal ring canals (D. N. R. and L. C., unpublished data). The mutant phenotype and the immunolocalization of the hts product suggest that hts plays a direct role in the establishment of actin on the inner rim on the ring canal. The homology of the amino-half of the predicted product of the *hts* cDNA to vertebrate adducin (Yue and Spradling, 1992; Ding et al., 1993) makes it tempting to speculate that hts interacts with ring canal actin through the adducin domain. However, there are several reasons to conclude that the hts ring canal protein does not contain the adducin domain. The ring canal staining antibodies were generated against the carboxy-half of the hts protein that does not share homology with any known protein. These antibodies recognize a doublet of proteins at 60×10^3 M_r by western blot, which is much smaller than the 128×10^3 M_r predicted by the *hts* cDNA (Yue and Spradling, 1992; Ding et al., 1993). Polyclonal antibodies raised to the adducin domain fail to recognize the 60×10^3 M_r doublet and instead recognize a 140×10^3 M_r protein (D. N. R. and L. C., unpublished data).

The 60×10^3 M_r proteins and the 140×10^3 M_r protein are likely to be encoded by distinct mRNAs. DNA probes that include the adducin domain hybridize to three transcripts (4.4 kb, 3.8 kb and 3.7 kb) that are expressed throughout development, including in the ovary (Yue and Spradling, 1992; D. N. R. unpublished data). Probes to the carboxy (ring canal) domain hybridize to a single ovary-specific 4.4 kb transcript (D. N. R., unpublished data), the cDNA of which has been sequenced (Yue and Spradling, 1992; Ding et al., 1993). Since the carboxy domain DNA probe recognizes a single transcript, the 60×10^3 M_r ring canal proteins must be produced from this known *hts* cDNA (Yue and Spradling, 1992; Ding et al., 1993). Therefore, it is possible that the 60×10^3 M_r ring canal protein arises from proteolysis of a precursor protein encoded by the known *hts* cDNA. Peptide sequences of the 60×10^3 M_r proteins are required to confirm the origin and nature of the hts ring canal protein. Actin binding assays with the hts ring canal protein might confirm that it is a new type of actin binding protein.

Products of the *hts* gene are important at other stages of development. In addition to containing defective ring canals,

hts mutants also disrupt the formation of the fusome normally present in mitotic germline cells in the germarium (Lin et al., 1994). Antibodies to the adducin portion of the *hts* cDNA immunostain the fusome as well as the membranes of follicle cells surrounding egg chambers (D. N. R. and L. C., unpublished data; Lin et al., 1994). The hts protein in fusomes and cell membranes is probably functionally similar to vertebrate adducin, serving to stabilize the cortical cytoskeleton. Finally, some alleles of *hts* have a maternal effect lethal phenotype (Yue, 1992) that may be related to the unusual anterior localization of *hts* mRNA in oocytes late in oogenesis (Yue and Spradling, 1992; Ding et al., 1993).

The last protein we have found to be recruited to ring canals is kelch. It accumulates after the ring canal is established and is essential for maintenance of ring canal rim structure. In a *kelch* mutant ring canal, both hts and actin protein distributions are disorganized, and the proteins fail to compact (Fig. 6). This suggests that kelch interacts with actin or hts directly to organize or bundle actin into the neatly packed inner rim of the ring canal. An interaction with actin may be mediated by the carboxy-terminal kelch repeats. The gene for the *Limulus* actin binding protein, scruin (Tilney, 1975), was cloned and found to encode two sets of six kelch repeats, one in the amino-terminal half and the second in the carboxy-terminal half (Way and Matsudaira, personal communication). Ultrastructural analysis of *Limulus* sperm actin bundles (Owen and DeRosier, 1993; Schmid et al., 1994) shows that the repeat domains bind adjacent actin monomers in a filament. The carboxy-terminal repeat domain may be responsible for bundling since it appears to associate with a carboxy-terminal repeat domain of a scruin molecule in a neighboring actin filament (Bullitt et al., 1988). By analogy, it is probable that kelch binds to an actin filament through its repeat domain and could also provide a bundling function. The morphology of *kelch* mutant ring canals supports the idea that kelch is providing a bundling function. Actin filaments in *kelch* mutant ring canals are distributed in the lumen of the canal, sometimes appearing to form a smaller ring suspended within the canal lumen. In the absence of kelch, any remaining actin filament bundling proteins might bundle actin filaments inappropriately in a loose meshwork. The absence of kelch may even allow the binding of actin binding proteins not normally found in ring canals. This could result in a substantially different filament crosslinking pattern that accounts for the diffuse appearance of actin in *kelch* mutants.

In *kelch* mutant ring canals, both hts and actin appear to be present in increased amounts (Fig. 6) suggesting another possible function for kelch. kelch may limit actin polymerization on the ring canal rim by capping growing filaments or by sterically limiting actin polymerization. However, we cannot rule out the possibility that ring canal assembly and growth require a carefully regulated balance between the different ring canal protein levels. Loss of one of these (for example, kelch) may perturb this balance resulting in aberrant ring canal morphology.

The failure to complete cytoplasm transport to the oocyte in *kelch* mutant females (Xue and Cooley, 1993) can now be attributed to occluded ring canals. The transport defect appears to begin early in the vitellarium at the same time that the disorganization of hts and actin on the inner rims of ring canals first becomes apparent. The partially occluded ring canals do not block all transport because some mRNAs and proteins that are transported at specific times in egg chamber development still arrive on time in *kelch* mutants (D. N. R. and L. C., unpublished data). Oocyte growth in *kelch* mutant egg chambers is retarded perhaps because the mutant ring canal cannot permit passage of larger cytoplasmic components such as mitochondria or because the mutant ring canal cannot accommodate the enormous volume of cytoplasm necessary for oocyte maturation.

Conclusion

Cytoplasmic bridges provide important intercellular connections between developing gametes of many invertebrate and vertebrate organisms. We have gained insight into the development and structure of germline ring canals in *Drosophila* females. We expect ring canal structure is somewhat different in males since both hts and kelch are absent from the testis (D.N.R., unpublished data). Perhaps the transport of cytoplasm to a selected cell in female syncytia places a special structural burden on the intercellular junctions. Ultrastructural similarities between female ring canals of insects and mammals, in addition to the presence of a possible *kelch* homolog in mouse (MIPP), suggest that mammalian ring canals might be similar to *Drosophila* ring canals. It is possible that the sequential addition of proteins to a stabilized cleavage furrow during the formation of a ring canal may be a recurring theme found in other systems. Additional genetic and biochemical analyses of *Drosophila* ring canal proteins and a study of homologous proteins in the mouse are needed to determine the degree of conservation of this fascinating structure.

We thank Lin Yue for *hts* cDNAs; David Ward and members of his laboratory for use of the confocal microscope and imaging equipment; Michael Sepanski and Haifan Lin for electron microscopy; Dennis McKearin and Allan Spradling for comments on the manuscript; and Michael Way and Paul Matsudaira for sharing unpublished results. This work was supported by grants from the NIH and the Pew Charitable Trusts (L. C.) and an NIH predoctoral training grant (D. N. R.), and an NIH Medical Scientist Training Program grant (K.C.)

REFERENCES

Anderson, E. and Huebner, E. (1968). Development of the oocyte and its accessory cells of the polychaete, *Diopatra cuprea* (Bosc). *J. Morph.* **126**, 163-198.

Brown, E. H. and King, R. C. (1964). Studies on the events resulting in the formation of an egg chamber in Drosophila melanogaster. *Growth* **28**, 41-81.

Bullitt, E. S. A., DeRosier, D. J., Coluccio, L. M. and Tilney, L. G. (1988). Three-dimensional reconstruction of an actin bundle. *J. Cell Biol.* **107**, 597-611.

Burgos, M. H. and Fawcett, D. W. (1955). Studies on the fine structure of the mammalian testis. *J. Biophysic. Biochem. Cytol.* **1**, 287-300.

Burridge, K., Fath, K., Kelly, T., Nuckolls, G. and Turner, C. (1988). Focal adhesions: Transmembrane junctions between the extracellular matrix and the cytoskeleton. *Ann. Rev. Cell Biol.* **4**, 487-525.

Cant, K., Knowles, B., Mooseker, M. and Cooley, L. (1994). Drosophila singed, a fascin homolog, is required for actin bundle formation during oogenesis and bristle extension. *J. Cell Biol.* **125**, 369-380.

Chang-Yeh, A., Mold, D. E. and Huang, R. C. C. (1991). Identification of a novel murine IAP-promoted placenta-expressed gene. *Nucl. Acids Res.* **19**, 3667-3672.

Cooley, L., Verheyen, E. and Ayers, K. (1992). *chickadee* encodes a profilin required for intercellular cytoplasm transport during Drosophila oogenesis. *Cell* **69**, 173-184.

DiBello, P. R., Withers, D. A., Bayer, C. A., Fristrom, J. W. and Guild, G.

M. (1991). The Drosophila *Broad-Complex* encodes a family of related proteins containing zinc fingers. *Genetics* **129**, 385-397.

Ding, D., Parkhurst, S. M. and Lipshitz, H. D. (1993). Different genetic requirements for anterior RNA localization revealed by the distribution of adducin-like transcripts during Drosophila oogenesis. *Proc. Nat. Acad. Sci. USA* **90**, 2512-2516.

Dyer, R. F., Ruby, J. R. and Skalko, R. G. (1968). Intercellular bridges between developing mouse oocytes. *J. Cell Biol.* **39**, 38a.

Franchi, L. L. and Mandl, A. M. (1962). The ultrastructure of oogonia and oocytes in the foetal and neonatal rat. *Proc. Roy. Soc. B* **157**, 99-114.

Fujiwara, K., Porter, M. E. and Pollard, T. D. (1978). Alpha-actinin localization in the cleavage furrow during cytokinesis. *J. Cell Biol.* **79**, 268-275.

Godt, D., Couderc, J.-L., Cramton, S. E. and Laski, F. A. (1993). Pattern formation in the limbs of Drosophila: *bric à brac* is expressed in both a gradient and a wave-like pattern that is required for specification and proper segmentation of the tarsus. *Development* **119**, 799-812.

Gondos, B. (1973). Intercellular bridges and mammalian germ cell differentiation. *Differentiation* **1**, 177-182.

Gutzeit, H. (1986a). The role of microtubules in the differentiation of ovarian follicles during vitellogenesis in Drosophila. *Roux's Arch. Dev. Biol.* **195**, 173-181.

Gutzeit, H. O. (1986b). The role of microfilaments in cytoplasmic streaming in Drosophila follicles. *J. Cell Sci.* **80**, 159-169.

Harrison, S. D. and Travers, A. A. (1990). The *tramtrack* gene encodes a Drosophila finger protein that interacts with the *ftz* transcriptional regulatory region and shows a novel embryonic expression pattern. *EMBO J.* **9**, 207-216.

Harlow, E. and Lane, D. (eds) (1988). *Antibodies: A Laboratory Manual*, pp. 53-43. Cold Spring Harbor, NY: Cold Spring Harbor Laboratory Press.

King, R. C. and Mills, R. P. (1962). Oogenesis in adult Drosophila. XI. Studies of some organelles of the nutrient stream in egg chambers of D. melanogaster and D. willistoni. *Growth* **26**, 235-253.

King, R. C. and Storto, P. D. (1988). The role of the *otu* gene in Drosophila oogenesis. *Bioessays* **8**, 18-24.

Koch, E. A. and King, R. C. (1966). The origin and early differentiation of the egg chamber of *Drosophila melanogaster*. *J. Morph.* **119**, 283-304.

Koch, E. A. and King, R. C. (1969). Further studies on the ring canal system of the ovarian cystocytes of Drosophila melanogaster. *Z. Zellforsch.* **102**, 129-152.

Koonin, E. V., Senkevich, T. G. and Chernos, V. I. (1992). Protein sequence motifs: A family of DNA virus genes that consists of fused portions of unrelated cellular genes. *Trends Biochem. Sci.* **17**, 213-214.

Laemmli, U. K. (1970). Cleavage of structural proteins during the assembly of the head of bacteriophage T4. *Nature* **227**, 680-685.

Lin, H., Yue, L. and Spradling, A. (1994). The Drosophila fusome, a germline-specific organelle, contains membrane skeletal proteins and functions in cyst formation. *Development* **120**, 947-956.

Lindsley, D. L. and Zimm, G. G. (1992). *The Genome of Drosophila Melanogaster*. San Diego: Academic Press, Inc.

Mahowald, A. and Strassheim, J. (1970). Intercellular migration of centrioles in the germarium of Drosophila melanogaster: An electron microscopic study. *J. Cell Biol.* **45**, 306-320.

Mahowald, A. P. (1971). The formation of ring canals by cell furrows in Drosophila. *Z. Zellforsch.* **118**, 162-167.

Mahowald, A. P. and Kambysellis, M. P. (1980). Oogenesis. In *The Genetics and Biology of Drosophila* vol. 2D (eds M. Ashburner and T. Wright) pp. 141-224. New York: Academic Press.

Meyer, G. F. (1961). Interzelluläre brücken (fusome) in hoden und im einährzellverband von Drosophila melanogaster. *Z. Zellforsch.* **54**, 238-251.

Owen, C. and DeRosier, D. (1993). A 13-Å map of the actin-scruin filament from the Limulus acrosomal process. *J. Cell Biol.* **123**, 337-344.

Sanger, J. M., Mittal, B., Pochapin, M. B. and Sanger, J. W. (1987). Stress fiber and cleavage furrow formation in living cells microinjected with fluorescently labeled alpha-actinin. *Cell Motil.* **7**, 209-220.

Sato, N., Yonemura, S., Obinata, T., Tsukita, S. and Tsukita, S. (1991). Radixin, a barbed end-capping actin-modulating protein, is concentrated at the cleavage furrow during cytokinesis. *J. Cell Biol.* **113**, 321-330.

Satterwhite, L. L. and Pollard, T. D. (1992). Cytokinesis. *Curr. Opin. Cell Biol.* **4**, 43-52.

Schmid, M. F., Agris, J. M., Jakana, J., Matsudaira, P. and Chiu, W. (1994). Three-dimensional structure of a single filament in the Limulus acrosomal bundle: Scruin binds to homologous helix-loop-beta motifs in actin. *J. Cell Biol.* **124**, 341-350.

Senkevich, T. G., Muravnik, G. L., Pozdnyakov, S. G., Chizhikov, V. E., Ryazankina, O. I., Shchelkunov, S. N., Koonin, E. V. and Chernos, V. I. (1993). Nucleotide sequence of Xho I O fragment of ectromelia virus DNA reveals significant differences from vaccinia virus. *Virus Res.* **30**, 73-88.

Smith, D. B. and Johnson, K. S. (1988). Single-step purification of polypeptides expressed in Escherichia coli as fusions with glutathione S-transferase. *Gene* **67**, 31-40.

Spradling, A. (1993). Developmental genetics of oogenesis. In *The Development of Drosophila melanogaster* vol. 1 (eds M. Bate and A. Martinez Arias), pp. 1-70. Cold Spring Harbor, NY: Cold Spring Harbor Laboratory Press.

Storto, P. D. and King, R. C. (1988). Multiplicity of functions for the *otu* gene products during Drosophila oogenesis. *Dev. Genet.* **9**, 91-120.

Theurkauf, W., Alberts, B., Jan, Y. and Jongens, T. (1993). A central role for microtubules in the differentiation of *Drosophila* oocytes. *Development* **118**, 1169-1180.

Tilney, L. G. (1975). Actin filaments in the acrosomal reaction of Limulus sperm. *J. Cell Biol.* **64**, 289-310.

Towbin, H., Staehelin, T. and Gordon, J. (1979). Electrophoretic transfer of protein from polyacrylamide gels to nitrocellulose sheets: procedures and applications. *Proc. Nat. Acad. Sci. USA* **76**, 4350-4354.

Tsukita, S., Hieda, Y. and Tsukita, S. (1989). A new 82-kD barbed end-capping protein (radixin) localized in the cell-cell adherens junction: purification and characterization. *J. Cell Biol.* **108**, 2369-2382.

Volberg, T., Geiger, B., Dror, R. and Zick, Y. (1991). Modulation of intercellular adherens-type junctions and tyrosine phosphorylation of their components in RSV-transformed cultured chick lens cells. *Cell Regul.* **2**, 105-120.

Volberg, T., Zick, Y., Dror, R., Sabanay, I., Gilon, C., Levitzki, A. and Geiger, B. (1992). The effect of tyrosine-specific protein phosphorylation on the assembly of adherens-type junctions. *EMBO J.* **11**, 1733-1742.

Warn, R., Gutzeit, H., Smith, L. and Warn, A. (1985). F-actin rings are associated with the ring canals of the Drosophila egg chamber. *Exp. Cell Res.* **157**, 355-363.

Weakley, B. S. (1967). Light and electron microscopy of developing germ cells and follicle cells in the ovary of the golden hamster: twenty four hours before birth to eight days post partum. *J. Anat.* **101**, 435-459.

Xue, F. and Cooley, L. (1993). *kelch* encodes a component of intercellular bridges in Drosophila egg chambers. *Cell* **72**, 681-693.

Yue, L. (1992). Genetic and molecular characterization of *hu-li tai shao* (*hts*), a gene required for ring canal formation during Drosophila oogenesis. Ph.D. Thesis, Johns Hopkins University: Baltimore, MD.

Yue, L. and Spradling, A. (1992). *hu-li tai sha*o, a gene required for ring canal formation during Drosophila oogenesis, encodes a homolog of adducin. *Genes Dev.* **6**, 2443-2454.

Zamboni, L. and Gondos, B. (1968). Intercellular bridges and synchronization of germ cell differentiation during oogenesis in the rabbit. *J. Cell Biol.* **36**, 276-282.

(Accepted 12 April 1994)